analytical chemistry

Article

pubs.acs.org/ac

Relative Quantification in Imaging of a Peptide on a Mouse Brain Tissue by Matrix-Assisted Laser Desorption Ionization

Kyung M. Park,[†] Jeong H. Moon,[‡] Kwang P. Kim,[§] Seong H. Lee,[†] and Myung S. Kim*[,†]

[†]Department of Chemistry, Seoul National University, Seoul 151-747, Korea

[‡]Medical Proteomics Research Center, KRIBB, Daejeon 305-806, Korea

[§]Department of Applied Chemistry, Kyunghee University, Yongin 446-701, Korea

Supporting Information

ABSTRACT: It is well-known that the number of analyte ions generated by matrix-assisted laser desorption ionization (MALDI) is not directly proportional to the analyte concentration at the irradiated spot. This is an obstacle to acquiring quantitatively meaningful maps for materials in a tissue by MALDI imaging. The problem worsens as the matrix suppression due to contaminants in the sample increases. In this work, we use a peptide as an example and show that we can overcome this problem by utilizing three guidelines derived from our recent studies on the generation of reproducible MALDI spectra. First is to acquire MALDI spectra under a temperature-controlled condition. Second is to keep the matrix suppression below an experimentally determined limit, and the third is to construct the image map using the peptide-to-matrix ion abundance ratio rather than the peptide ion abundance. The strategy works well for contaminated tissue samples and generates quantitatively meaningful maps. Also, it is demonstrated that a preposterous map can be generated when the peptide ion abundance is used in the construction of the map.

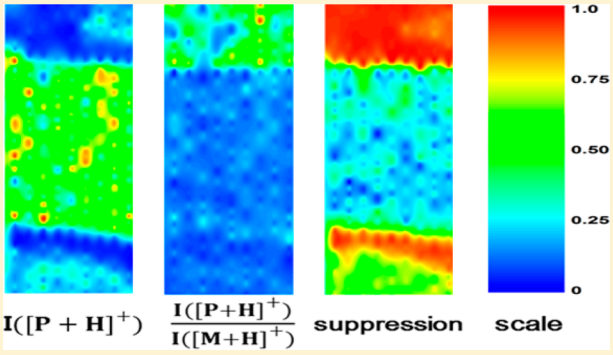

Determining the spatial distributions of biological or pharmaceutical molecules in tissue samples is of current interest.[1−6] Imaging methods based on mass spectrometry (mass spectrometric imaging, MSI)[3−6] are particularly attractive because of its capability to identify analyte molecules. Here, mass spectra generated by a technique for gas-phase ion formation from samples in condensed phases are acquired at many locations on a tissue. Then, the abundances of an ion with a particular mass-to-charge ratio are plotted in the form of a two-dimensional image map. Secondary ion mass spectrometry (SIMS)[7,8] and matrix-assisted laser desorption ionization (MALDI)[9,10] are two popular ion formation techniques that are widely used in MSI, especially in combination with time-of-flight (TOF) mass analysis. Compared to SIMS, MALDI is more useful for generating molecular ions of large labile biological molecules.[5] On the other hand, the spatial resolution in MALDI is poorer than in SIMS. Progresses are being made to lessen the weaknesses of each technique.

In the interpretation of MALDI imaging data, it is implicitly presumed[11] that the abundance of an ion measured at a particular location increases with the amount of the corresponding analyte molecule at the same two-dimensional location in the original tissue. This assumption consists of two preconditions. First is that the amount of the analyte available for ionization at a particular two-dimensional location is a good representation of its amount at the same location inside the original tissue. Second is that the measured ion abundance increases with the amount of the analyte. It is to be noted that, if the rule governing the relation between the amount of an analyte and the measured ion abundance, this pertains to the second assumption, is unknown, even the validity of the first assumption cannot be checked. Recently, it was reported that the chemical environment of an analyte also affected the measured ion abundance, which is often called "ion suppression".[12,13] With severe ion suppression in MALDI at a spot, an ion signal might be difficult to observe even when a large amount of the corresponding analyte is present at the spot, a case against the utility of MSI.

For many years, it was widely thought that ion signals generated by MALDI were irreproducible, from sample to sample, from spot to spot in a sample, and from shot to shot at a spot.[14,15] Hence, development of the current MALDI-based MSI[16] that can generate reproducible images in favorable cases should be regarded as a real achievement, although there is no guideline to check the quantitative validity of such images.

Recently,[17] we found that the overall pattern of and the abundance of each ion appearing in the MALDI-TOF spectrum of a peptide became reproducible when the effective temperature, T_{early},[18] in the early plume where the in-source decay[19] occurred was kept constant. We also found[20] that the matrix-to-

Received: March 12, 2014
Accepted: April 24, 2014
Published: April 24, 2014

   dx.doi.org/10.1021/ac500911x | *Anal. Chem.* 2014, 86, 5131−5135

peptide proton transfer occurring in the plume was in quasi-equilibrium and resulted in the following relation.

$$I([P + H]^+)/I([M + H]^+) = KI(P)/I(M) \quad (1)$$

Here, I represents the abundance of a matrix (M)- or peptide (P)-derived species in the plume and K is the equilibrium constant. $I(P)/I(M)$ in the plume was taken to be the same as the corresponding ratio, or peptide concentration, in the solid sample. Direct proportionality between $I([P + H]^+)/I([M + H]^+)$ and $I(P)/I(M)$ in eq 1 is essentially a calibration relation that can be used for the quantification of the peptide.[20] It is to be emphasized that the peptide concentration in the solid sample is proportional to $I([P + H]^+)/I([M + H]^+)$, not to the peptide ion abundance, $I([P + H]^+)$, itself. Also to be emphasized is that eq 1, which is an equilibrium relation, will hold even when other reactions also occur in the plume and are in quasi-equilibrium. We found[21] that the linear relation in eq 1 held as long as the matrix suppression, S, was small, e.g., 70% or less when α-cyano-4-hydroxycinnamic acid (CHCA) was the matrix.

$$S = 1 - I([M + H]^+)/I_0([M + H]^+) \quad (2)$$

Here, $I_0([M + H]^+)$ is the matrix ion abundance in MALDI of the pure matrix.

Our quantification method for peptides by MALDI is based on two pillars, i.e., acquisition of spectra at a constant T_{early} and their analysis with eq 1. The method was tested for various samples of matrix-peptide mixtures loaded on stainless steel targets.[20,21] In this work, we will show that the method also works for the relative quantification of peptides in samples loaded on mouse brain tissues.

EXPERIMENTAL SECTION

All the measurements were made with a home-built MALDI-tandem TOF apparatus described previously.[22] The apparatus consists of an ion source with delayed extraction, an ion gate, a reflectron, and a microchannel plate detector just as for most conventional instruments. The accelerating voltage in the source is 21.5 kV. 337 nm output from a nitrogen laser (MNL100, Lasertechnik Berlin, Berlin, Germany) is focused on the sample to an ellipse with the semimajor (y) and semiminor (z) axes of ~65 and ~25 μm, respectively. The area of a peak in a mass spectrum was taken as the relative abundance of the corresponding ion. This was converted to the number of ions by taking into account the detector gain.[23] Operation of the instrument including temperature control and data acquisition and processing were carried out by homemade software.

As mentioned earlier, MALDI spectra of a sample become reproducible when the temperature in the early plume, T_{early}, is kept constant. As measures of T_{early}, we initially utilized the extent of fragmentation of a peptide ion or a matrix ion.[18,20] Later,[24] we observed that the total number of particles hitting the detector (loosely called total ion count or TIC) was a good measure of T_{early}. The method to keep T_{early} constant is as follows.[24] For a fresh sample, we measure the threshold pulse energy for MALDI. This is ~0.4 μJ per pulse when CHCA is the matrix. Typically, we begin spectral acquisition using two times the threshold pulse energy. TIC measured for a fresh sample at this pulse energy is ~1500 counts per pulse, which is taken as the preset value. As the irradiation at a spot continues, T_{early} goes down and hence TIC decreases. Then, we raise the pulse energy to bring TIC back to the preset value. Eventually, depleted regions begin to appear on the irradiated spot, typically when the pulse energy increases to three times the threshold.

In a typical imaging experiment, 50 and 10 spots along the y and z axes, respectively, were chosen at the interval of 150 μm. From the data collected at many spots, an image map was constructed using a commercial software (Origin, version 8.0, Northampton, MA, USA). Using the same data, we also estimated the thickness distribution of the matrix layer on a tissue. The method to estimate the thickness is described in the Supporting Information. We did not use data from a spot when the matrix thickness there was far off from the average.

Reagents and Sample Preparation. Peptides Y_5R and YLYEIAR were purchased from Peptron (Daejeon, Korea). All the other chemicals were purchased from Sigma (St. Louis, MO, USA).

Five μm thick mouse brain tissues[25] were prepared following the method in ref 26. Two different procedures, Procedure I and II, were used to clean the tissues. In Procedure I, a tissue was dipped twice in 7:3 ethanol/water for 30 s. In Procedure II, a tissue treated by Procedure I was further dipped twice in 100% ethanol for 30 s. Naturally, the tissues prepared by Procedure II were cleaner.

Sample solutions containing CHCA and peptides were prepared with 1:1 acetonitrile/water. A commercial device (ImagePrep, Bruker Daltonik GmbH, Bremen, Germany) was used to spray-coat a tissue with a sample solution. The protocol recommended by the manufacturer for spraying CHCA solution was used.

RESULTS AND DISCUSSION

Principle of the Method. The strategy we adopted to estimate the relative amount of a peptide at a spot from ion signals in MALDI is as follows. (1) Implicitly, it is thought that a fairly even thickness of matrix layer throughout a tissue is a requirement for reliable imaging. As mentioned in the previous section, we estimated the thicknesses of the matrix layer at each spot and used it as a measure of sample quality (in the Supporting Information). (2) TIC is kept constant throughout the measurement for a tissue sample. As shown in an earlier report,[27] K and the amount of materials ablated per laser shot that is essentially $I(M)$ in eq 1 are constant when TIC is kept constant. Then, when the thickness of the matrix layer is similar throughout the sample, the number of single-shot spectra that can be acquired from each spot would be similar. (3) With $I(M)$ and K kept constant, eq 1 for the ith shot at a spot becomes as follows.

$$I_i([P + H]^+)/I_i([M + H]^+) = KI_i(P)/I(M) \quad (3)$$

Summing over the total number of shots at a spot and rearranging, eq 3 is converted as follows.

$$I_{total}(P) = \{I(M)/K\} \sum_i \{I_i([P + H]^+)/I_i([M + H]^+)\} \quad (4)$$

Here, I_{total} (P) represents the total amount of the peptide at the spot where the measurement has been made. Equation 4 tells us that this is proportional to $\Sigma_i\{I_i([P + H]^+)/I_i([M + H]^+)\}$ measured at the spot, not to $\Sigma_i I_i([P + H]^+)$. $\Sigma_i I_i([P + H]^+)$ does not increase as rapidly as the peptide concentration because the amount of the matrix ion in the plume is reduced due to the matrix-to-peptide proton transfer. That is, "ion suppression" occurs by way of "matrix suppression". (4) An

dx.doi.org/10.1021/ac500911x | Anal. Chem. 2014, 86, 5131−5135

analyte ion signal may also be suppressed due to salts and basic contaminants.[5,28] Previously,[21] we showed that we could handle the matrix suppression by basic contaminants by using eq 1 and by keeping the matrix suppression low, e.g., 70% or less when CHCA was the matrix. So far, we have not reported any result concerning the influence of the contamination by salts on the quantification of peptides. The fact that the matrix suppression by salts can also be handled by eq 1 is shown in the Supporting Information.

Relative Quantification of a Peptide Loaded on a Mouse Brain Tissue. Earlier, we pointed out that a quantitative imaging by MALDI was hampered by two problems, one concerned with the analyte transfer from tissue to matrix layer and the other with MALDI of the analyte in the matrix layer. In this paper, we would like to demonstrate that the method we developed for peptide quantification by MALDI, i.e., maintaining TIC constant, keeping the suppression low, and using eq 1, can solve the second problem. To avoid complications that might be caused by the first problem, we decided to analyze a peptide that had been spray-coated on a tissue together with a matrix rather than those that had originated from the tissue.

We first prepared tissues displaying very small matrix suppression by cleaning them according to Procedure II described in the Experimental Section. We spray-coated a cleaned tissue with CHCA, acquired its MALDI spectrum, and compared it with a similar spectrum acquired from an uncleaned tissue (not shown). The abundances of $[CHCA + Na]^+$ at m/z 212 and of a lipid-derived ion at m/z 184 were very small in the former spectrum compared to those in the latter spectrum. Instead, the matrix-derived ions of $[CHCA + H]^+$, $[CHCA + H - H_2O]^+$, $[CHCA + H - CO_2]^+$, and $[2CHCA + H]^+$ got prominent, indicating very small suppression. Using tissues cleaned by Procedure II, we prepared two samples, tissues A and B, by spray-coating them with 1:1 acetonitrile/water containing 25 nmol of CHCA per μL and Y_5R. The concentrations of Y_5R in solutions used to prepare tissues A and B were 1.5 and 15 pmol μL^{-1}, respectively. MALDI spectra acquired from tissues A and B are shown in Figure 1a,b, respectively. We evaluated $\Sigma_i I_i([P + H]^+)$ and $\Sigma_i\{I_i([P + H]^+)/I_i([M + H]^+)\}$ and took their averages for each tissue. The results are shown in Table 1.

As the concentration of Y_5R increased by a factor of 10 from tissue A to tissue B, $\Sigma_i I_i([P + H]^+)$ increased only by a factor of 4.3 (p value of 3×10^{-14}). In contrast, $\Sigma_i\{I_i([P + H]^+)/I_i([M + H]^+)\}$ increased in proportion to the peptide concentration ($p = 0.61$). We also performed similar experiments for another tissue, to be called tissue C, which was intentionally contaminated as follows. We cleaned a tissue by Procedure II, loaded 4 μL of a solution containing 200 pmol of YLYEIAR at one edge, dried it, spray-coated it with a solution containing 25 nmol of CHCA and 1.5 pmol of Y_5R per μL, and took the MALDI spectra at several spots in the contaminated region. Here, Y_5R is playing the role of the analyte while YLYEIAR is playing that of a contaminant. From the sets of spectra we acquired, we evaluated $\Sigma_i I_i([P + H]^+)$ and $\Sigma_i\{I_i([P + H]^+)/I_i([M + H]^+)\}$ for Y_5R. Their averages are listed in Table 1. The peptide-to-matrix ion abundance ratios measured for tissues A and C are similar ($p = 0.21$) while the total peptide ion abundances are not ($p = 1 \times 10^{-17}$). The above data suggest that the ion abundance ratio is a good representation of the peptide concentration at any location on a tissue while the peptide ion abundance is not.

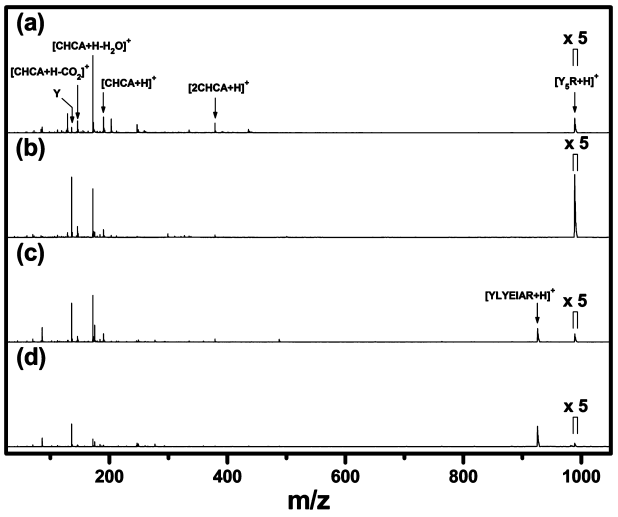

Figure 1. MALDI spectra of Y_5R acquired from tissues prepared in various ways. We cleaned each tissue by Procedure II. Spectra (a) and (b) were acquired from tissues that were spray-coated with a solution containing 25 nmol of CHCA per μL and 1.5 and 15 pmol per μL of Y_5R, respectively. Both spectra (c) and (d) were acquired from regions contaminated by YLYEIAR. To acquire spectra (c) and (d), 4 μL of a solution containing 200 and 600 pmol of YLYEIAR, respectively, was loaded at one location on the tissue. After the solvent evaporation, the tissue was spray-coated with a solution containing 25 nmol of CHCA and 1.5 pmol of Y_5R per μL.

Table 1. Analyte (Y_5R) Signals from Mouse Brain Tissues Spray-Coated with a Solution Containing 25 nmol μL^{-1} of CHCA, Y_5R, and a Peptide Contaminant

tissue	Y_5R concentration (pmol μL^{-1})	contaminant	$\Sigma_i I_i([P + H]^+)$[a]	$\Sigma_i\{I_i([P + H]^+)/I_i([M + H]^+)\}$
A	1.5		4000 ± 1200	1.4 ± 0.4
B	15		17000 ± 5000	14 ± 4.1
C[b]	1.5	YLYEIAR	1400 ± 500	1.6 ± 0.5

[a]In arbitrary units. [b]Data evaluated from the spectra acquired from a region contaminated by YLYEIAR.

Image Distortion Due to Matrix Suppression. To observe the influence of matrix suppression on MALDI image maps, we performed the following two experiments for Y_5R on tissue samples. In the first experiment, Y_5R and YLYEIAR were taken as the analyte and the contaminant, respectively. The method to prepare a tissue sample is as follows. We cleaned a tissue by Procedure II and contaminated it by loading 4 μL of a solution containing 200 pmol of YLYEIAR at one (bottom) edge of the tissue and the same volume of a solution containing 600 pmol of the same peptide at the opposite (top) edge. Each volume spread out to a circle with around 2 mm in diameter. After the solvent had evaporated, the tissue surface was spray-coated with a solution containing 1.5 pmol of Y_5R and 25 nmol of CHCA per μL. MALDI spectra acquired under the TIC control from spots near the bottom (lightly contaminated) and top (heavily contaminated) edges are shown in Figure 1c,d, respectively. Comparing Figure 1a,c, one finds that the matrix suppression by YLYEIAR somewhat reduces the abundances of all the matrix-derived ions. However, the matrix suppression near the bottom edge is not severe, only around 60%. In contrast, all the CHCA-derived ions become very weak in Figure 1d. Dominant ions in this spectrum are mostly

dx.doi.org/10.1021/ac500911x | Anal. Chem. 2014, 86, 5131−5135

YLYEIAR-derived. The matrix suppression in Figure 1d estimated from the abundances of $[CHCA + H]^+$ in Figure 1a,d is 95%, which is larger than our guideline of 70%.

In Figure 2a, a color-coded image map constructed with the peptide ion abundances ($\Sigma_i I_i([P + H]^+)$) measured at many

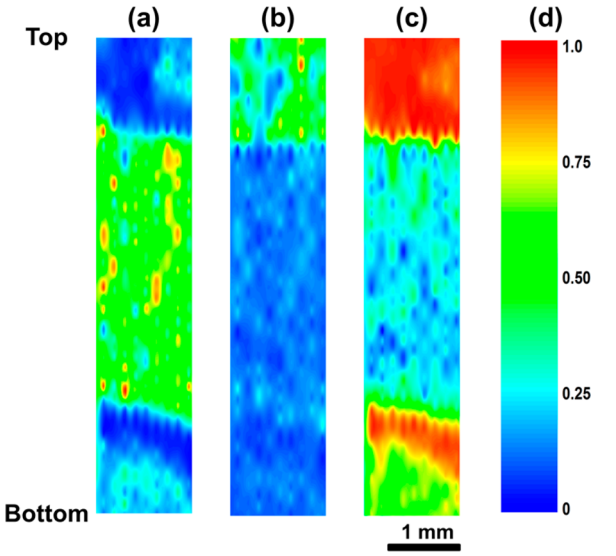

Figure 2. Image maps of Y_5R on a tissue that was spray-coated with a solution containing CHCA and Y_5R. The tissue was contaminated by larger (near the top edge) and smaller (near the bottom edge) amounts of YLYEIAR. Image maps were constructed with (a) $\Sigma_i I_i([P + H]^+)$ and (b) $\Sigma_i\{I_i([P + H]^+)/I_i([M + H]^+)\}$. (c) is the suppression (eq 2) map. To draw (a), $\Sigma_i I_i([P + H]^+)$ at each spot was normalized to the largest value in the map and color-coded according to the scale in (d). (b) was drawn similarly. To draw (c), matrix suppression at each spot was color-coded to the scale in (d).

spots on the tissue is shown. The peptide ion abundance at each spot was normalized to the largest value observed. A similar map constructed with the peptide-to-matrix ion abundance ratio is shown in Figure 2b. Finally, a matrix suppression map (eq 2) is shown in Figure 2c. In this figure, the matrix suppression near the top edge is larger than in the bottom edge, as mentioned above.

The image map for Y_5R constructed with the peptide ion abundance, Figure 2a, indicates that the tissue is roughly divided into three parts, top, middle, and bottom, that have small, medium, and small amounts of Y_5R, respectively. This is in disagreement with our expectation that the concentration of Y_5R would be the same throughout the sample. In the image map constructed with the peptide-to-matrix ion abundance ratio, Figure 2b, the amount of Y_5R in the bottom part becomes comparable to that in the middle part, in agreement with our expectation. On the other hand, the amount of Y_5R in the top part appears larger than in the other parts, in disagreement with our expectation. Looking at the suppression map in Figure 2c, however, one realizes that the image distortion in the top part has arisen due to high matrix suppression: depending on the peptide analyzed, the peptide-to-matrix ion abundance ratio can be larger or smaller than the correct value (ref 20).

Matrix suppression by materials originating from the tissue can also distort an image map. Amounts of such materials in a sample may vary depending on the cleaning procedure used. In our second experiment, we first cleaned a tissue by Procedure I. Then, one part (bottom) of the tissue was dipped twice in 100% ethanol for 30 s. That is, the bottom part of the tissue was cleaned by Procedure II while the top part was cleaned by Procedure I. At the top edge of the tissue, we loaded 6 μL of a solution containing 100 pmol of Y_5R. Then, we spray-coated the whole tissue with a solution containing 25 nmol of CHCA and 1.5 pmol of Y_5R per μL. In the matrix suppression map, Figure 3c, drawn from the spectral data acquired for this sample, matrix suppression near the top part is 50−90%, which is larger than 5−40% near the bottom part, as expected.

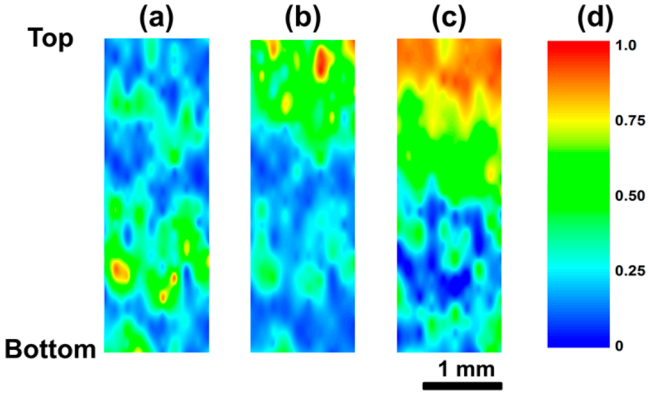

Figure 3. Influence of the tissue cleaning procedure on the image map of Y_5R. The top and bottom parts of a tissue were cleaned by Procedures I and II, respectively. Six μL of a solution containing 100 pmol of Y_5R was loaded near the top edge. Finally, the whole tissue was spray-coated with a solution containing 1.5 pmol of Y_5R and 25 nmol of CHCA per μL. (a) and (b) are image maps constructed with $\Sigma_i I_i([P + H]^+)$ and $\Sigma_i\{I_i([P + H]^+)/I_i([M + H]^+)\}$, respectively. (c) is the suppression map. (d) shows the scale used in color-coding.

The image map constructed with the peptide ion abundance, Figure 3a, indicates that the concentration of Y_5R in the top part is smaller than that in the bottom part. This is in disagreement with our expectation. In contrast, the image map constructed with the peptide-to-matrix ion abundance ratio, Figure 3b, predicts higher concentration of Y_5R near the top edge, which is likely because the matrix suppression near the top part is mostly smaller than 70%. That is, the suppression map constructed with the imaging data can be a useful guideline to check the relative quantitativeness of the image map.

■ CONCLUSION

Although MALDI imaging is a powerful technique for visualizing the presence of certain materials at particular locations on a tissue, a method to construct a quantitatively meaningful image map from experimental data is not available yet. In this work, we demonstrated that such maps could be constructed by adopting the peptide-to-matrix ion abundance ratio as the measure of the analyte concentration at the spot rather than the analyte ion abundance itself. Acquisition of spectral data at a fixed effective temperature was one of the requirements. Even the peptide-to-matrix ion abundance ratio might not be a reliable measure of the peptide concentration in the region where the sample is heavily contaminated by salts and/or by bases. Then, the matrix suppression map drawn from imaging data can be a useful guideline to check the quantitative reliability of the image map. We may enhance the relative quantitativeness of the map through a reduction of the matrix suppression by cleaning the tissue or by diluting the analyte.

dx.doi.org/10.1021/ac500911x | *Anal. Chem.* 2014, 86, 5131−5135

■ ASSOCIATED CONTENT

Supporting Information

Additional information as noted in the text. This material is available free of charge via the Internet at http://pubs.acs.org.

■ AUTHOR INFORMATION

Corresponding Author

*E-mail: myungsoo@snu.ac.kr.

Notes

The authors declare no competing financial interest.

■ ACKNOWLEDGMENTS

This work was supported by the National Research Foundation of Korea (NRF) grant funded by the Korean government (MEST) (2013076408).

■ REFERENCES

(1) Salzer, R.; Siesler, H. W. *Infrared and Raman Spectroscopic Imaging*; Wiley-VCH: Weinheim, 2009.
(2) Ntziachristos, V. *Annu. Rev. Biomed. Eng.* **2006**, *8*, 1−33.
(3) Caprioli, R. M.; Farmer, T. B.; Gile, J. *Anal. Chem.* **1997**, *69*, 4751−4760.
(4) Cornett, D. S.; Reyzer, M. L.; Chaurand, P.; Caprioli, R. M. *Nat. Methods* **2007**, *4*, 828−833.
(5) Chughtai, K.; Heeren, R. M. A. *Chem. Rev.* **2010**, *110*, 3237−3277.
(6) Nemes, P.; Vertes, A. *Anal. Chem.* **2007**, *79*, 8098−8106.
(7) Benninghoven, A.; Rudenauer, F. G.; Werner, H. W. *Secondary Ion Mass Spectrometry: Basic Concepts, Instrumental Aspects, Applications and Trends*; Wiley-Interscience: Hoboken, 1987.
(8) Mahoney, C. M. *Mass Spectrom. Rev.* **2010**, *29*, 247−293.
(9) Hillenkamp, F.; Peter-Katalinić, J. *MALDI MS. A practical guide to instrumentation, methods and applications*; Wiley-VCH: Weinheim, 2007.
(10) Cole, R. B. *Electrospray and MALDI mass spectrometry. Fundamentals, instrumentation, practicalities, and biological applications*, 2nd ed.; Wiley: Hoboken, 2010.
(11) Chaurand, P.; Schwartz, S. A.; Caprioli, R. M. *Anal. Chem.* **2004**, *76*, 86A−93A.
(12) Heeren, R. M. A.; Kükrer-Kaletaş, B.; Taban, I. M.; MacAleese, L.; McDonnell, L. A. *Appl. Surf. Sci.* **2008**, *255*, 1289−1297.
(13) Lanni, E. J.; Rubakhin, S. S.; Sweedler, J. V. *J. Proteomics* **2012**, *75*, 5036−5051.
(14) Duncan, M. W.; Roder, H.; Hunsucker, S. W. *Briefings Funct. Genomics Proteomics* **2008**, *7*, 355−370.
(15) Pirman, D. A.; Reich, R. F.; Kiss, A.; Heeren, R. M. A.; Yost, R. A. *Anal. Chem.* **2013**, *85*, 1081−1089.
(16) Puolitaival, S. M.; Burnum, K. E.; Cornett, D. S.; Caprioli, R. M. *J. Am. Soc. Mass Spectrom.* **2008**, *19*, 882−886.
(17) Bae, Y. J.; Park, K. M.; Kim, M. S. *Anal. Chem.* **2012**, *84*, 7107−7111.
(18) Yoon, S. H.; Moon, J. H.; Kim, M. S. *J. Am. Soc. Mass Spectrom.* **2010**, *21*, 1876−1883.
(19) Hardouin, J. *Mass Spectrom. Rev.* **2007**, *26*, 672−682.
(20) Park, K. M.; Bae, Y. J.; Ahn, S. H.; Kim, M. S. *Anal. Chem.* **2012**, *84*, 10332−10337.
(21) Ahn, S. H.; Bae, Y. J.; Moon, J. H.; Kim, M. S. *Anal. Chem.* **2013**, *85*, 8796−8801.
(22) Bae, Y. J.; Yoon, S. H.; Moon, J. H.; Kim, M. S. *Bull. Korean Chem. Soc.* **2010**, *31*, 92−99.
(23) Moon, J. H.; Yoon, S. H.; Kim, M. S. *J. Phys. Chem. B* **2009**, *113*, 2071−2076.
(24) Ahn, S. H.; Park, K. M.; Bae, Y. J.; Kim, M. S. *J. Am. Soc. Mass Spectrom.* **2013**, *24*, 868−876.
(25) Sugiura, Y.; Shimma, S.; Setou, M. *J. Mass Spectrom. Soc. Jpn.* **2006**, *54*, 45−48.
(26) Shanta, S. R.; Zhou, L. H.; Park, Y. S.; Kim, Y. H.; Kim, Y. J.; Kim, K. P. *Anal. Chem.* **2011**, *83*, 1252−1259.
(27) Bae, Y. J.; Choe, J. C.; Moon, J. H.; Kim, M. S. *J. Am. Soc. Mass Spectrom.* **2013**, *24*, 1807−1815.
(28) Aerni, H. R.; Cornett, D. S.; Caprioli, R. M. *Anal. Chem.* **2006**, *78*, 827−834.